A New Strategy of Fc-recognizable Peptide Ligand Design for Oriented Immobilization of Antibody.

ARTICLE *in* ANALYTICAL CHEMISTRY · FEBRUARY 2014

Impact Factor: 5.64 · DOI: 10.1021/ac4029467 · Source: PubMed

4 AUTHORS, INCLUDING:

Wen-Yih Chen
National Central University
140 PUBLICATIONS **2,436** CITATIONS

SEE PROFILE

analytical chemistry

Article

pubs.acs.org/ac

Strategy of Fc-Recognizable Peptide Ligand Design for Oriented Immobilization of Antibody

Ching-Wei Tsai,[†] Siang-Long Jheng,[†] Wen-Yih Chen,[†,‡] and Ruoh-Chyu Ruaan*[,†,‡]

[†]Department of Chemical and Materials Engineering, National Central University, Chung-Li City, Taoyuan 32001, Taiwan

[‡]Institute of Biomedical Engineering, National Central University, Chung-Li City, Taoyuan 32001, Taiwan

ABSTRACT: A new strategy for designing a short-chain peptide ligand with high affinity to the Fc region of an antibody was proposed. The targeted antibody is human prostate specific antibody (PSA) derived from Mouse IgG_{2a}. The ligand design strategy involves two major parts: binding site selection and peptide ligand design. One of the exposed hydrophobic patches near the bottom of the antibody's Fc region, identified from the molecular docking of naphthelene and end-capped tryptophan, was selected as the binding site. After examining the charge distribution around the binding site, various peptide ligands were designed according to the possible hydrophobic and electrostatic interactions. A peptide ligand, RRGW, was found to have high Fc binding affinity by the analysis of molecular dynamics (MD) simulation. The first two residues, two arginines, play an important role in electrostatic interaction between the peptide and the Fc region of the antibody. The fourth residue, the tryptophan, provides the VDW force; and the flexibility of peptide is achieved through the help of the third residue, the glycine. The binding affinity, recognition efficiency, and orientation factor were calculated from the results of surface plasmon resonance (SPR) measurements. The result shows that the dissociation constant is 5.56×10^{-10} M^{-1}. We also found that the recognition efficiency and orientation factor on the ligand attached surface were much higher than those on negatively and positively charged surfaces. This approach provides a simple and fast strategy for small ligands design on oriented antibody immobilization.

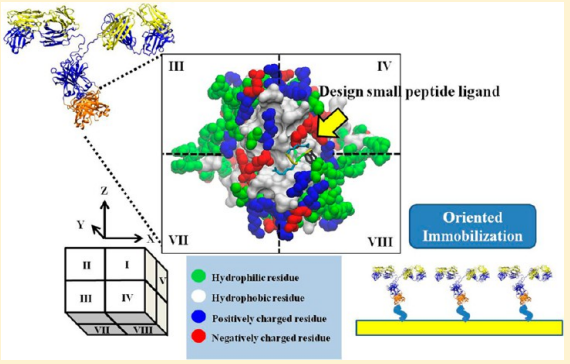

Protein immobilization technology has been widely applied to various biochemical assays and biotransformation processes.[1−6] Most protein immobilization techniques result in protein attachment in various orientations, which cause considerable activity loss. Oriented immobilization was proposed to increase the efficiency of biotransformation and to enhance the sensitivity of bioassays.[7−12] Immunosensors and immunoassays based on specific bioaffinity interaction between antibody and antigen to detect pathogens, toxicants, or specific markers in complex mixtures are the most important diagnostic tools for applying in disease diagnostics, environmental analysis, and translational medicine, etc.[13] The recognition sensitivity of immunosensors is strongly dependent on the sensitivity of the signal-sensing mechanism, the amount of immobilized antibody on the chip surface, and the orientation of the immobilized antibody. However, while biological molecules were immobilized on the sensor surface, the control over the orientation of the immobilized antibody has not so far been fully achieved.[14] Apparently, the signal would be significantly reduced due to the random orientation of antibody on the chip surface.

Three major techniques have been adopted for oriented immobilization of antibodies. One is to introduce reduction reagent to detach the Fab fragments through the disulfide linkages and then immobilize the fragments through the reduced thiol groups.[15] Kausaite-Minkstimien et al. have compared the different antibody immobilization techniques for modification on the surface plasmon resonance (SPR) chip. They found the immobilization of Fab fragments is the most suitable for design of the SPR-immunosensor for antibody detection, due to the sufficient antigen binding capacity, simplicity, and low cost in respect to the currently evaluated techniques.[16] This means that the immobilized technique based on Fab fragments is much more stable than the whole IgG, but unfortunately the Fab fragments tend to form aggregates in solution. Another method is to chemically attach biotin or single strand DNA to the antibody and the affinity counterpart, avidin or complementary DNA, to the chip surface.[17] Antibodies are then immobilized through bioaffinity. Fan et al. have developed the integrated blood barcode chip using this technique.[18] The other method is to chemically attach protein A or protein G to the chip surface.[19,20] Protein A and protein G have high affinity for the polysaccharide region of the antibodies, which were immobilized through their polysaccharides in Fc regions. Except for the protein A and protein G, Kwon et al. have examined that the immobilized cutinase on the surface can immobilize the antibody to detect the specific antigen in a complex mixture.[21] The other protein-mediated end-point immobilization was also facilitated by sortase.[22,23] All the methods mentioned above involved chemically modifying

Received: September 16, 2013
Accepted: February 16, 2014

   dx.doi.org/10.1021/ac4029467 | *Anal. Chem.* XXXX, XXX, XXX−XXX

antibodies or protein ligands covalently binding to a chip surface. Antibodies or protein ligands, however, may be partially denatured during these chemical processes, which significantly diminish the advantages of oriented immobilization. As a result, Jung et al. have proposed a strategy to immobilize an antibody on various sensor surfaces by using a small antibody-binding peptide, where they suggested that the antibody-binding peptide conjugate may offer a highly stable and specific surface platform for antibody immobilization in immunoassays.[24]

In this study we proposed a new strategy to design small affinity peptide ligands for oriented immobilization of antibodies. The small ligand is covalently bound to the chip surface and designed to grasp onto a specific spot on the bottom of the Fc region of the antibody by involving the hydrophobic and electrostatic interactions. First, molecular docking of benzene and end-capped tryptophan molecule are performed to rank the possible hydrophobic sites on the surface of Fc region. The most hydrophobic spot near the bottom of Fc region is selected as the target binding site. Second, we analyzed the charged amino acids distribution near the target binding site. The electrostatic interactions near hydrophobic patches are much stronger due to the entropy gain from the repelling bound water around a hydrophobic patch.[25−29] Peptide ligands are designed to match the charges and hydrophobic distribution of the target binding site. Third, molecular dynamics simulation is performed to find the most suitable ligand. The ligand having the highest affinity to the target site and low affinity to other hydrophobic sites is chosen.

The targeted antibody is human prostate specific antibody (PSA) derived from Mouse IgG_{2a}. The recognition efficiency and oriented factor of Mouse IgG_{2a} with the designed peptide ligand are determined by surface plasmon resonance (SPR) measurement. Mixed self-assembled monolayer (SAM) of two alkanethiolates is chemically attached to the Au coated SPR chip. The peptide ligand is then covalently bound to the carboxyl ended alkanethiolates. The specific PSA adsorption and orientation factor are measured and compared with those on randomly adsorbed surfaces, i.e., positively and negatively charged surfaces. On the other hand, the normal PSA concentration in human serum is about 0.1−2.6 ng/mL and the warning point is about 10 ng/mL. Thus, we also measured the sensitivity of PSA detection by our designed peptide ligand. The result revealed that the PSA could be detected even when the concentration of PSA declines to 2 ng/mL.

MATERIALS AND METHODS

Chemical Components. The 1-ethyl-3-(3-dimethylaminopropyl)-carbodiimide hydrochloride (EDC), 2-(*N*-morpholino)ethanesulfonic acid sodium salt (MES), trifluoroacetic acid (TFA), absolute ethanol (99.5%), 2-aminoethanol, bovine serum albumin (BSA), and lysozyme (LYZ, from chicken egg whites) were purchased from Sigma-Aldrich (U.S.). The sodium phosphate dibasic anhydrous, sodium phosphate monobasic monohydrate, and ethanol were purchased from J. T. Baker (U.S.). The *N*-hydroxy-sulfo-succinimide (sulfo-NHS) was purchased from Thermo (U.S.). The OEG-terminated thiols [$HSC_{11}(EG)_6OCH_2COOH$ and $HSC_{11}(EG)_6OH$] were purchased from ProChimia (Poland). Mouse antihuman prostate specific antigen and prostate specific antigen were purchased from US Biological (U.S.). The goat anti-Mouse IgG_{2a} was purchased from Jackson ImmunoResearch (U.S.). The ethylenediamine was purchased from Alfa Aesar (England). The customized synthesis peptide ligand, Arg-Arg-Gly-Trp-NH_2, was obtained from Kelowna International Scientific Inc., Taiwan.

Molecular Docking. The rigid docking calculations of the protein-hydrophobic probe were performed to search for the exposed hydrophobic patch of the Fc region by the AutoDock Program (version 4.0.1). Two hydrophobic probes, naphthalene and end-capped tryptophan, were used. The conformation of IgG2a was derived from the X-ray diffraction results (PDB code: 1IGT). The conformation of naphthalene was obtained with the AM1 method by using the Gaussian 03 program for the energy minimization. The end-caped tryptophan (N-terminal actylation and C-terminal amidation) was constructed from the CHARMM program. AutoDock Tools (ADT) 4.0 was used for the addition of polar hydrogen and assign partial atomic charges with Kollman charges for antibody and hydrophobic probes. The atom type was assigned by ATD 4.0. The docking calculations were performed by Genetic Algorithms. All the configuration figures were visualized by the VMD software.[30]

Molecular Dynamics Simulation. The peptide-antibody binding energy and configuration were determined by implicit solvent molecular dynamics (MD) simulations. All peptide ligands were constructed with extended structure by CHARMM Software (c35b5).[31] The potential function of peptide and protein were modeled using CHARMM-22 force filed. The GBMV method was carried out for implicit solvation calculation. Briefly, the designed peptide ligand was initially put 10 Å away from the selected binding site of the Fc region. We fixed the heavy atom of main chain (Cα, N, C, O) of antibody and let the side chain of antibody be flexible during the simulation. The simulation temperature was maintained at the experimental temperature of 298 K. Cutoffs of 18 Å were used to calculate the pairwise interactions and generate the list of pairs, and the nonbonded neighboring list was updated every 20 steps. The SHAKE algorithm was used to constrain the hydrogen atom-involved covalent bonds. The integration time step is 1 fs. Before MD simulation, 2500 steps of energy minimization were performed to remove the bad contacts of the initial models. The visualization of the atomic configurations and the analysis of interaction energy were determined by VMD software. The implicit MD simulation was run for 2 ns. Average energies were calculated from the last 0.2 ns of MD simulation.

Mixed SAM Preparation and Ligand Attachment. Three functionalized surfaces were fabricated on the SPR sensor chip. The negatively charged surface was prepared by a mixing SAM of $HS(CH_2)_{11}(EG)_6OCH_2COOH$ and $HS(CH_2)_{11}(EG)_4OH$ with a 1:10 ratio.[32] The positively charged and peptide ligand bound surfaces were obtained by amidation the carboxyl groups of the mixing SAM with ethylenediamine and peptide ligand, respectively. The SPR sensor chips were prepared by coating a gold layer (48 nm) via a sputtering deposition process at pressure below 1×10^{-6} Torr on the clean BK7 glass substrates which were precoated with 2 nm of chromium adhesion layer. Before preparing the mixing SAMs, we first clean the gold chip by ultraviolet−ozone treatment for 20 min, followed by the ethanol and distilled deionized water (DI-H_2O) wash for three times. Then, we put the chip in 20 mL of ethanol solution containing of the mixture of OEG-/COOH-OEG-terminated thiol with the final concentration of 1 mM. After reacting for 16 h, we immersed the chip in 1% (v/v) TFA/EtOH to avoid the multilayer formation.[33] Finally, the negatively charged surface was fabricated after rinsing the chip

dx.doi.org/10.1021/ac4029467 | Anal. Chem. XXXX, XXX, XXX−XXX

with an ethanolic solution of NH_4OH (10%, v/v) and DI-H_2O. On the other hand, the positively charged surface was fabricated by grafting the ethylenediamine (EDA) to the carboxyl group on the OEG-/COOH-OEG-terminated mixing SAM using the EDC/NHS activation method. We immersed the chip into the 0.1 M pH 6.0 MES buffer containing 200 mM EDC and 50 mM NHS at 25 °C for 0.5 h. After washing the chip by DI-H_2O, the chip was further immersed in the pH 7.4 PBS buffer containing of 5 mM EDA for 2 h. The unreacted carboxyl groups on the SAM surface were blocked by 20 mM ethanolamine. The positively charged surface was washed by DI-H_2O and characterized by XPS analysis. The N/O ratio is 0.26 which approximates to the theoretical value (0.25). The third modified surface is the peptide ligand grafting surface. Similarly, we used the EDC/NHS activation method to graft RRGW-NH_2 peptide on the OEG-/COOH-OEG-terminated mixing SAM. The activation procedure is the same as the modification of the positively charged surface. Then, we put the carboxyl group activated chip in the peptide solution with the concentration of 5 mM in pH 7.4 PBS buffer for 2 h. The unreacted carboxyl groups on the SAM surface were also blocked by ethanolamine. Finally, the chip was washed by DI-H_2O.

Surface Plasmon Resonance Analysis. The amounts of antibody and antigen adsorption on the negatively charged, positively charged, and peptide-grafted chips were determined by a custom built SPR sensor.[28] SPR signals are highly sensitive in refractive index change as the protein interacts with the sensing surface. Freshly prepared SAMs and modified chips were used for all SPR experiments. All SPR measurements were operated under a flow rate of 20 μL/min at 25 °C. The adsorption of IgG_{2a} was performed with the concentration of 10 μg/mL in 10 mM phosphate buffer (PB), pH 7.4. The concentrations of the second antibody (Goat anti-Mouse IgG_{2a}) and PSA were 10 and 5 μg/mL, respectively. The adsorption operation condition was met by first pumping the PB into the flow cell for 15 min and then switching from the PB to IgG_{2a} for 60 min. Following the IgG_{2a} adsorption, the desorption process were conducted by switching back to the PB at the flow rate of 20 μL/min for 170 min. Finally, the antigen or secondary antibody was pumped for 60 min then the nonspecific protein adsorption was washed by PB over 30 min. The addition of 0.3% NaCl increased the refractive index of the running buffer with 4.68×10^{-5} refractive index units (RIU). The SPR signal change (ΔdB) could be in terms of the amounts of protein adsorption per cm^2 based on the above buffer calibration.[34] The recognition efficiency is defined by the ratio of the amount of antigen to the antibody binding. The orientation factor was defined by the ratio of the amount of primary to secondary antibodies binding. To examine the sensitivity of immobilized IgG_{2a} on the peptide ligand (RRGW) modified surface, we first flowed the 10 μg/mL IgG_{2a} on the peptide modified chip for 30 min and then switched to PB buffer for 30 min. Second, we pumped the PSA in different concentrations (2, 5, 10 ng/mL) into the flow cell for 30 min and then switched from PB to IgG2a for 30 min. Following the IgG_{2a} adsorption, the desorption process were conducted by switching back to the PB at the flow rate of 20 μL/min for 30 min. The amount of IgG2a adsorption in the second time was plotted as a function of PSA concentration to obtain the sensitivity of PSA detection. All the SPR measurements were performed three times, and the average values and standard deviations were reported.

RESULTS AND DISCUSSION

The Fc-recognizable peptide ligand with high affinity toward the Fc region of antibody was designed through the hydrophobic and electrostatic attractive interactions between the peptide ligand and the Fc region of the antibody. With the optimal binding orientation of the antibody, antigen recognition efficiency may be enhanced. The proposed strategy of peptide ligand design adopts the following steps: (1) Search for a possible peptide ligand binding site through the help of molecular docking. (2) Design the peptide ligand according to the analysis of pocket size and surface amino acid functionality around the set site. (3) Screen the high affinity peptide ligand by molecular dynamics simulation. Finally, the designed Fc-recognizable peptide ligand was immobilized on the SPR chip surface, and the SPR sensor was used to determine the antigen recognition efficiency and orientation factor.

Searching Possible Binding Sites on Fc Region. Before designing a high affinity peptide ligand to bind with the Fc region of antibody through the electrostatic and hydrophobic interactions, we first search the exposed hydrophobic surface at the lower Fc region to find a potential binding site. The center of mass of the lower part of Fc was set as (0, 0, 0), and we divided the region into eight octants. The V, VI, VII, and VIII octants were facing the bottom of the antibody (Figure 1A). Hydrophobic patches on the lower Fc region were searched

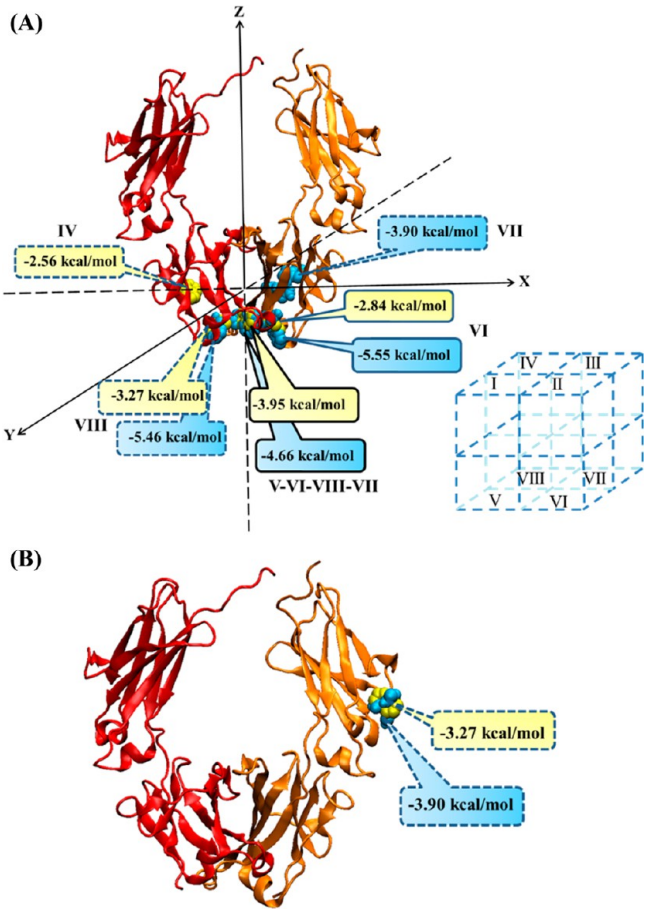

Figure 1. Binding energy and location of hydrophobic sites were identified by molecular docking using two hydrophobic probes: (A) lower Fc region and (B) upper Fc region. The yellow molecule is naphthalene, and the blue one is the end-capped tryptophan.

dx.doi.org/10.1021/ac4029467 | Anal. Chem. XXXX, XXX, XXX−XXX

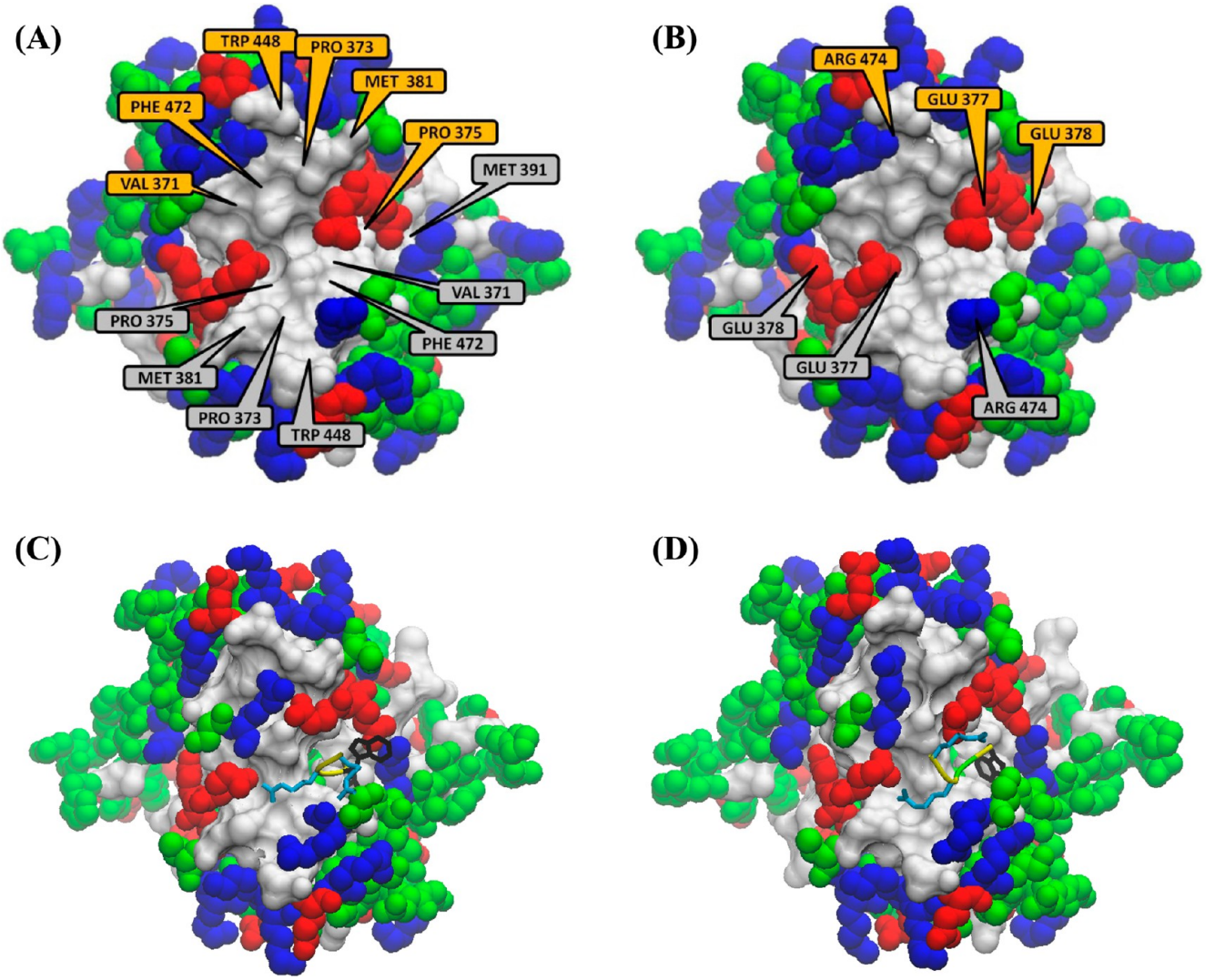

Figure 2. Amino acid distribution and peptide binding configuration in the selected binding site: (A) hydrophobic amino acids around the site, (B) charged amino acids around the site, (C) final binding posture of ligand RRWL, (D) final binding posture of ligand RRGW. The area in gray color represents the location occupied by hydrophobic amino acids. The area in blue marks the positively charged and the area in red marks negatively charged amino acids.

through the molecular docking of naphthalene and end-capped tryptophan by the AutoDock software. The four most hydrophobic sites were selected from the docking results of each hydrophobic probe.

Using end-capped tryptophan as the hydrophobic probe, only one of the hydrophobic docking sites is located in the VII octants and the other three docking sites located near the juncture of V, VI, VII, and VIII octants. Figure 1A showed that one of the most hydrophobic sites picked up by naphthalene is located in the IV octants and the other three located near the juncture of V, VI, VII, and VIII octants. The binding free energies calculated from molecular docking were also shown in Figure 1A. The most hydrophobic sites suggested by these two hydrophobic probes were all located near the bottom of the Fc region and the juncture of the V, VI, VII, and VIII octants. Therefore, we selected this area as the ligand binding area. Furthermore, we examined the charged amino acids in this area. As demonstrated in Figure 2A,B, this area is formed by two heavy chains. The hydrophobic patch contains Val 371, Met 381, Trp 448, and Phe 472 in both chains and two negatively charged Glu 377 on top of the patch. However, the electrostatic interactions near hydrophobic patches are much stronger due to the entropy gain from the repelling bound water around the hydrophobic patch.[25−29] Therefore, we suggested that the peptide ligands should contain hydrophobic and positively charged amino acids to exhibit high affinity with the ligand binding area.

Peptide Ligand Design Assisted by Molecular Dynamics Simulation. Peptide ligands were designed according to the distribution of hydrophobic and negatively charged amino acids in the binding site. Two types of end-capped peptide ligands were designed: hydrophobic/charged diblock and charged/hydrophobic/charged triblock ligands. The selected hydrophobic amino acids include Ile, Leu, Phe, and Trp. Also, the selected positively charged amino acids are Lys and Arg. To vary the block size, the ligands contain 3, 4, 5, or 7 residues. In total, 26 ligands were designed and their binding energies were determined by molecular dynamics simulation. The used the force field for the molecular dynamics simulation CHARMM PARA22. Atom motion was allowed only to the side chain of both heavy chains from residue 371 to 474. As our results, the triblock ligands were not to fit in the

dx.doi.org/10.1021/ac4029467 | Anal. Chem. XXXX, XXX, XXX−XXX

hydrophobic patch; it may be lower flexibility for the central hydrophobic part to bind with the surface exposed hydrophobic patch. Besides, we found that the ligands more than four residues were repelled from the binding site because of steric hindrance. While the ligands less than four residues show weak interaction with binding site. The four-residue diblock ligands possessed the highest affinity toward the binding site. We then compare the interaction free energies among these ligands. The van der Waals and electrostatic interaction energies were calculated for six of the four-residue diblock ligands. As shown in Table 1, end-capped RRWL appeared to have the strongest

Table 1. Interaction Energies between the Selected Binding Site and the Designed Four-Residue Peptide Ligands

peptide	electrostatic energy (kcal/mol)	Van der Waal energy (kcal/mol)	total energy (kcal/mol)
RRWW	−103.44	−50.20	−153.64
RRII	−108.59	−30.65	−139.24
RRLL	−91.84	−17.24	−109.08
RRLW	−130.87	−39.35	−170.23
RRWI	−81.95	−49.21	−131.16
RRWL	−128.49	−50.33	−178.81

interaction with the binding site. We further checked whether the interactions matched with our expectation. Figure 2C showed the final binding posture of RRWL. It was found that one of the arginine did not directly interact with the Glu in binding site. Energy analysis in Table 2 also showed low electrostatic energy contribution to one of the arginine, R1.

Table 2. Interaction Energy Contributed by Each Amino Acid of Ligand RRWL to the Selected Binding Site

residue	electrostatic energy (kcal/mol)	Van der Waal energy (kcal/mol)	total energy (kcal/mol)
R1	−41.51	−6.77	−48.28
R2	−90.02	−12.15	−102.17
W3	5.11	−13.82	−8.71
L4	−2.06	−17.58	−19.64
RRWL	−128.49	−50.33	−178.81

We, therefore, altered the design to RRGW for increasing ligand flexibility. Table 3 listed the calculated interaction energies. It could be observed that the total interaction energy decreases from −178.8 to −208.9 kcal/mol. The binding obviously becomes stronger even though one of the hydrophobic Lue is substituted by Gly. Figure 2D revealed the final posture of end-capped RRGW. Both arginines interacted with glutamines in the binding site, and the tryptophan is buried inside the hydrophobic cave.

From the surface hydrophobicity analysis, we obtained a hydrophobic patch located in the upper Fc. Figure 1B demonstrated the amino acid distribution and docking of hydrophobic probes. Both end-capped tryptophan and naphthalene molecules dock into this region. Glu 62 and Asp 91 of chain D are also nearby. To test the specificity of the designed ligand, we analyzed the binding of RRGW to this hydrophobic patch. From the analysis of MD simulation, we found that both van der Waals and electrostatic interactions are weak (Table 3), indicating the designed ligand is relatively specific to the target binding site.

Recognition Efficiency and Orientation Factor from the SPR Analysis. To test the applicability of the ligand, we compared the antibody adsorption, PSA adsorption, and secondary antibody adsorption of the ligand bound surface with the negatively and positively charged surfaces. To obtain the lower nonspecific binding surface, we have prepared the negatively charged surface which is composed of mixing the SAM of $HS(CH_2)_{11}(EG)_6OCH_2COOH$ and $HS-(CH_2)_{11}(EG)_4OH$ in a 1:10 ratio.[32] The positively charged and ligand bound surfaces were obtained by amidation of the carboxyl groups of the mixing SAM with ethylenediamine and peptide ligand, respectively. Bovine serum albumin and egg white lysozyme adsorption tests were performed on the negatively and positively charged surfaces. At the protein adsorption buffer condition with pH 7.4, the amount of BSA adsorption (15.4 ng/cm^2) was found much higher than that of LYZ (1.9 ng/cm^2) on the positively charged surface. The results reversed for BSA and LYZ adsorption on the negatively charged surface. The amounts of BSA and LYZ adsorption on the negatively charged surface is 1.5 ng/cm^2 and 3.4 ng/cm^2, respectively. The results indicate that the surfaces were properly modified.

The SPR signals of mouse IgG_{2a}, PSA, and secondary antibody adsorption on the three surfaces were shown in Figure 3A. It was found that the amount of mouse IgG_{2a} adsorption on the ligand attached surface is much higher than that on negatively and positively charged surfaces. The result may indicate high affinity between ligand and antibody or highly ordered immobilization of antibodies. The binding affinity of IgG_{2a} and RRGW peptide ligand is 1.8×10^9 M, which was calculated from a curve fitting.[28] By comparing the binding affinity of mouse IgG3 and that of cyclic peptide ligand (designed from Jung et al.),[24] the binding affinity of IgG_{2a} and our designed small peptide ligand is higher than that of mouse IgG3 and cyclic peptide ligand. Figure 3B showed the intensity of adsorption signals of PSA. The signal from the ligand attached surface is also much higher than that on negatively and positively charged surfaces. In particular, we found no significant PSA adsorption on the positively charged surface

Table 3. Interaction Energy Contributed by Each Amino Acid of Ligand RRGW to the Selected Binding Site and to the Hydrophobic Site on the Upper Fc Region

	at selected binding site			at hydrophobic site on upper Fc region		
residue	electrostatic energy (kcal/mol)	VDW energy (kcal/mol)	total energy (kcal/mol)	electrostatic energy (kcal/mol)	VDW energy (kcal/mol)	total energy (kcal/mol)
R1	−80.49	−6.05	−86.55	−19.43	−4.06	−23.49
R2	−74.06	−14.72	−88.78	−50.68	−9.39	−60.07
G3	−5.64	−5.15	−10.8	−2.97	−4.55	−7.52
W4	−0.59	−22.18	−22.78	0.64	−16.79	−16.15
RRGW	−160.79	−48.11	−208.9	−72.43	−34.8	−107.23

dx.doi.org/10.1021/ac4029467 | Anal. Chem. XXXX, XXX, XXX−XXX

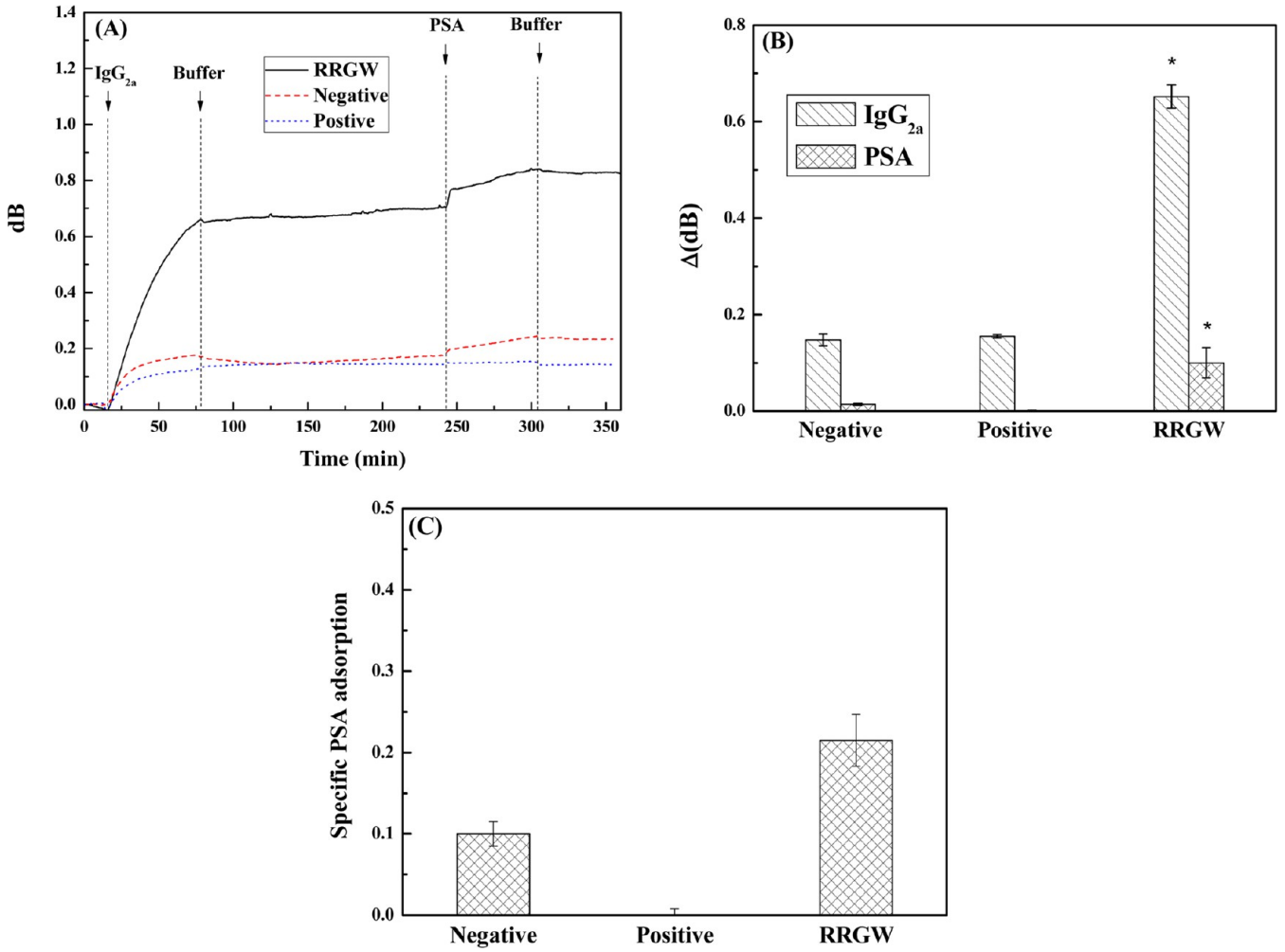

Figure 3. SPR signals of IgG_{2a} and PSA adsorption. (A) The overall spectra obtained from SPR measurements; (B) comparison of IgG_{2a} and PSA adsorption signals to the ligand attached, positively charged and negatively charged surfaces; (C) comparison of specific PSA adsorption to ligand attached, positively charged and negatively charged surfaces. Values are the means of three independent experiments; error bars represent s.d. (n = 3). Student's t test was performed; asterisks denote significance at a P value of <0.01 compared to the negatively charged surface.

(noting that the designed peptide ligands were also positively charged). The result suggested that the antibodies adsorb to the ligand mostly through the Fc regions but adsorb to positively charged surface mostly through the Fab. Dividing the PSA signal by IgG_{2a} signal, the specific PSA adsorption could be obtained. Figure 3C compared the recognition efficiency on the three surfaces. We find a higher amount of PSA adsorption on the ligand attached surface. The high specific PSA adsorption indicated that PSA was more accessible to the antibody adsorbed to the designed ligand than to the antibody on charged surfaces. We could expect that the ligand immobilized antibodies are more orderly oriented.

We further analyzed the orientation factor of IgG_{2a} adsorption. The orientation factor is defined by the binding ratio of primary to secondary antibodies. The SPR signals and intensity of adsorption signals of PSA were shown in Figure 4A,B, respectively. The primary antibodies were first introduced into the system. After washing with PB buffer, we further pumped the secondary antibodies in the cell. We finally washed out the nonspecific binding of secondary antibody. As shown in Figure 4C, we compared the orientation factors on the three surfaces. As expected, the ligand bound surface possessed the highest orientation factor, indicating that the ligand design is successful. However, the previous study has shown that the orientation factor of anti-CRP with peptide ligand is 0.191. The orientation factor of our designed peptide ligand is 0.48 which 2.5-times more effective than the previous study.[24] Furthermore, the recognition sensitivity of PSA on the peptide ligand modified surface was also measured by pumping the PSA concentration from 2 to 10 ng/mL. Then, we pumped the IgG_{2a} into the flow cell again. After washing the nonspecific binding antibody, the signals were recorded and plotted in Figure 5. The result showed that the PSA could be detected even when the concentration of PSA declines to 2 ng/mL. Therefore, the peptide ligand modified surface may be applied to the PSA disease diagnostics.

CONCLUSION

A new strategy for oriented immobilization of antibody was proposed. First, the hydrophobic spots on the surface of lower Fc region of the antibody were identified. One of the hydrophobic sites was selected as the binding site after evaluating the charge distribution. Affinity ligands were designed to maximize the hydrophobic and electrostatic interactions, and the ligand selection was assisted by molecular dynamics simulation. Peptide ligand RRGW was then selected

dx.doi.org/10.1021/ac4029467 | Anal. Chem. XXXX, XXX, XXX−XXX

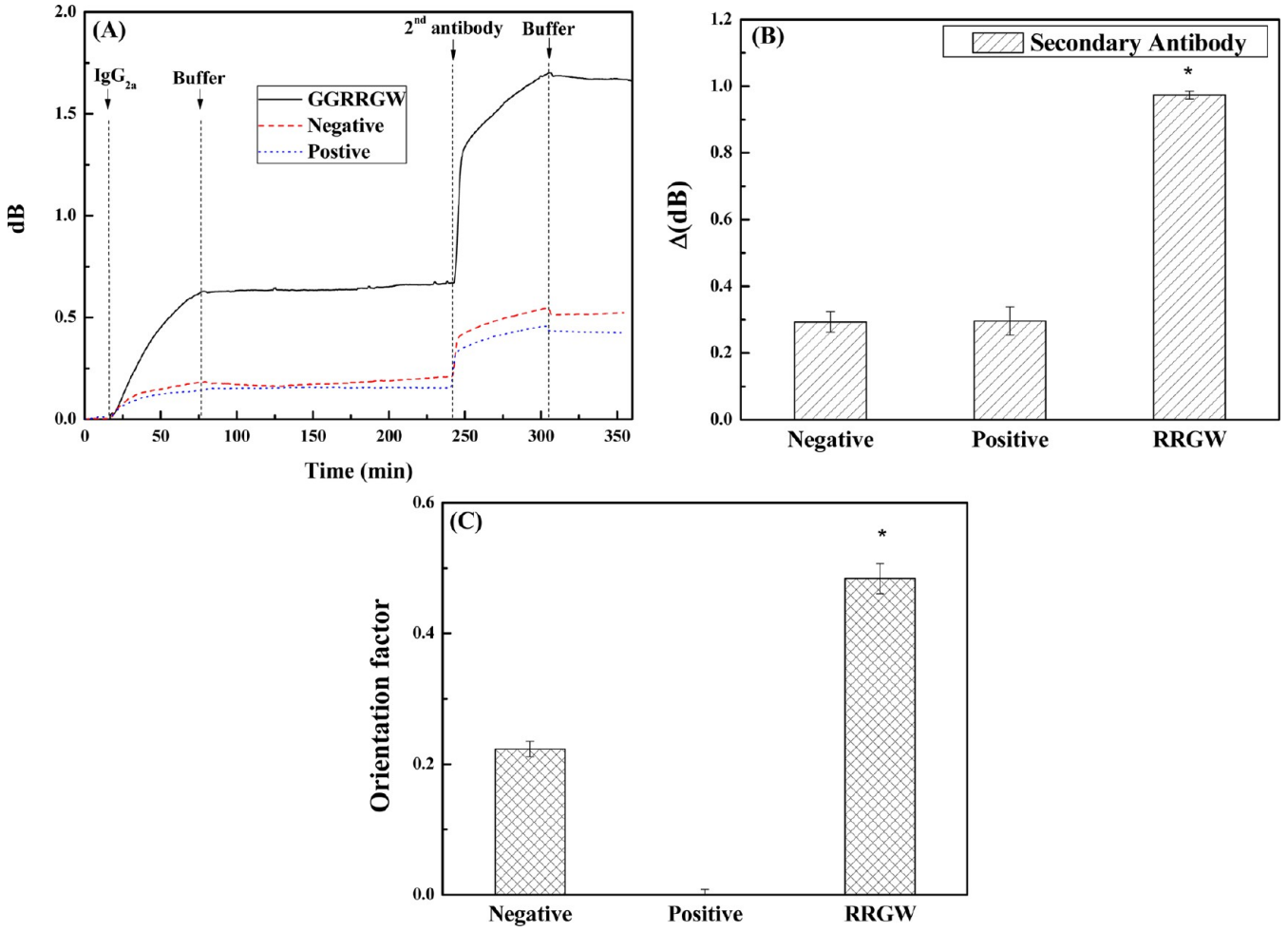

Figure 4. SPR signals of IgG_{2a} and 2nd antibody adsorption. (A) The overall spectra obtained from SPR measurements; (B) comparison of secondary antibody adsorption signals to the ligand attached, positively charged and negatively charged surfaces. (C) Comparison of specific orientation factors of mouse IgG_{2a} adsorption to the ligand attached, positively charged and negatively charged surfaces. Values are the means of three independent experiments; error bars represent s.d. (n = 3). Student's t test was performed; asterisks denote significance at a P value of <0.01 compared to the negatively charged surface.

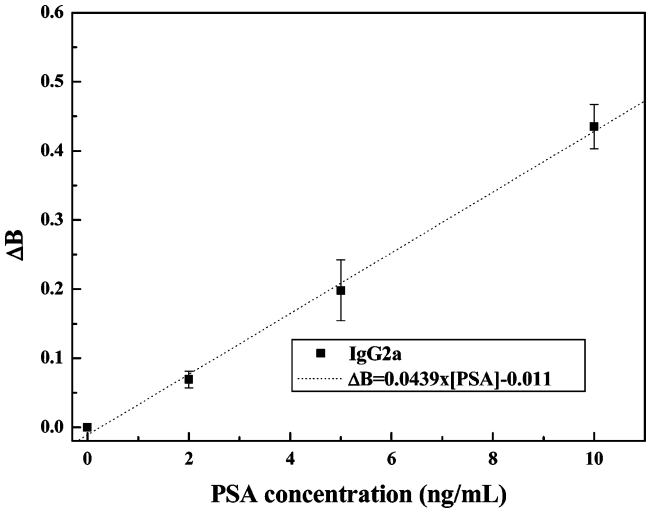

Figure 5. Sensitivity of RRGW-modified chip for PSA recognition by SPR measurement. Values are the means of three independent experiments; error bars represent s.d. (n = 3).

to target the selected binding site on Mouse IgG_{2a}. The affinity and immobilized orientation were evaluated by SPR. The high amount of IgG_{2a} adsorption, high specific adsorption of PSA, and high secondary antibody to the IgG_{2a} ratio indicate that the selected ligand owned high affinity toward the lower Fc region of IgG_{2a} and subsequently the immobilized antibodies were well oriented. We suggested that the proposed strategy is an easy and fast way for oriented immobilization of antibodies.

AUTHOR INFORMATION

Corresponding Author

*E-mail: ruaan@cc.ncu.edu.tw. Fax: +886-3-280-4341. Phone: +886-3-4227151#34232.

Notes

The authors declare no competing financial interest.

ACKNOWLEDGMENTS

The authors would like to thank the National Science Council (Grant Number 101-2221-E-008-088) of Taiwan for the financial support of this project. The authors also thank the National Center for High-Performance Computing of Taiwan and Vger Computer Cluster at National Center University of Taiwan for providing computer time and facilities.

REFERENCES

(1) Kacar, T.; Zin, M. T.; So, C.; Wilson, B.; Ma, H.; Gul-Karaguler, N.; Jen, A. K.; Sarikaya, M.; Tamerler, C. *Biotechnol. Bioeng.* **2009**, *103*, 696−705.

(2) Fang, Y.; Lahiri, J.; Picard, L. *Drug Discovery Today* **2004**, *9*, S61−67.

(3) Godl, K.; Wissing, J.; Kurtenbach, A.; Habenberger, P.; Blencke, S.; Gutbrod, H.; Salassidis, K.; Stein-Gerlach, M.; Missio, A.; Cotten, M.; Daub, H. *Proc. Natl. Acad. Sci. U.S.A.* **2003**, *100*, 15434−15439.

(4) Spiker, J. O.; Kang, K. A. *Biotechnol. Bioeng.* **1999**, *66*, 158−163.

(5) Forrer, P.; Tamaskovic, R.; Jaussi, R. *Biol. Chem.* **1998**, *379*, 1101−1111.

(6) Baniukevic, J.; Hakki Boyaci, I.; Goktug Bozkurt, A.; Tamer, U.; Ramanavicius, A.; Ramanaviciene, A. *Biosens. Bioelectron.* **2013**, *43*, 281−288.

(7) Liu, L.; Zheng, J.; Fang, G.; Xie, W. *Anal. Chim. Acta* **2012**, *726*, 85−92.

(8) Cho, I. H.; Park, J. W.; Lee, T. G.; Lee, H.; Paek, S. H. *Analyst* **2011**, *136*, 1412−1419.

(9) del Mar Garcia-Suarez, M.; Villaverde, R.; Gonzalez-Rodriguez, I.; Vazquez, F.; Mendez, F. J. *Curr. Microbiol.* **2009**, *59*, 81−87.

(10) Steinhauer, C.; Wingren, C.; Khan, F.; He, M.; Taussig, M. J.; Borrebaeck, C. A. *Proteomics* **2006**, *6*, 4227−4234.

(11) Mukhopadhyay, R.; Lo, K. K.; Wong, L. L.; Hill, H. A. *J. Microsc.* **2004**, *213*, 6−10.

(12) Puertas, S.; de Gracia Villa, M.; Mendoza, E.; Jimenez-Jorquera, C.; de la Fuente, J. M.; Fernandez-Sanchez, C.; Grazu, V. *Biosens. Bioelectron.* **2013**, *43*, 274−280.

(13) Ciani, I.; Schulze, H.; Corrigan, D. K.; Henihan, G.; Giraud, G.; Terry, J. G.; Walton, A. J.; Pethig, R.; Ghazal, P.; Crain, J.; Campbell, C. J.; Bachmann, T. T.; Mount, A. R. *Biosens. Bioelectron.* **2012**, *31*, 413−418.

(14) Iijima, M.; Somiya, M.; Yoshimoto, N.; Niimi, T.; Kuroda, S. *Sci. Rep.* **2012**, *2*, 790.

(15) Karyakin, A. A.; Presnova, G. V.; Rubtsova, M. Y.; Egorov, A. M. *Anal. Chem.* **2000**, *72*, 3805−3811.

(16) Kausaite-Minkstimiene, A.; Ramanaviciene, A.; Kirlyte, J.; Ramanavicius, A. *Anal. Chem.* **2010**, *82*, 6401−6408.

(17) Boozer, C.; Ladd, J.; Chen, S.; Yu, Q.; Homola, J.; Jiang, S. *Anal. Chem.* **2004**, *76*, 6967−6972.

(18) Fan, R.; Vermesh, O.; Srivastava, A.; Yen, B. K.; Qin, L.; Ahmad, H.; Kwong, G. A.; Liu, C. C.; Gould, J.; Hood, L.; Heath, J. R. *Nat. Biotechnol.* **2008**, *26*, 1373−1378.

(19) de Juan-Franco, E.; Caruz, A.; Pedrajas, J. R.; Lechuga, L. M. *Analyst* **2013**, *138*, 2023−2031.

(20) Jung, Y.; Lee, J. M.; Jung, H.; Chung, B. H. *Anal. Chem.* **2007**, *79*, 6534−6541.

(21) Kwon, Y.; Han, Z.; Karatan, E.; Mrksich, M.; Kay, B. K. *Anal. Chem.* **2004**, *76*, 5713−5720.

(22) Jiang, R.; Weingart, J.; Zhang, H.; Ma, Y.; Sun, X. L. *Bioconjugate Chem.* **2012**, *23*, 643−649.

(23) Popp, M. W.; Antos, J. M.; Grotenbreg, G. M.; Spooner, E.; Ploegh, H. L. *Nat. Chem. Biol.* **2007**, *3*, 707−708.

(24) Jung, Y.; Kang, H. J.; Lee, J. M.; Jung, S. O.; Yun, W. S.; Chung, S. J.; Chung, B. H. *Anal. Biochem.* **2008**, *374*, 99−105.

(25) Liu, C. I.; Hsu, K. Y.; Ruaan, R. C. *J. Phys. Chem. B* **2006**, *110*, 9148−9154.

(26) Huang, H. M.; Chen, W. Y.; Ruaan, R. C. *J. Colloid Interface Sci.* **2003**, *263*, 23−28.

(27) Huang, H. M.; Lin, F. Y.; Chen, W. Y.; Ruaan, R. C. *J. Colloid Interface Sci.* **2000**, *229*, 600−606.

(28) Tsai, C. W.; Ruaan, R. C.; Liu, C. I. *Langmuir* **2012**, *28*, 10446−10452.

(29) Tsai, C. W.; Liu, C. I.; Chan, Y. C.; Tsai, H. H.; Ruaan, R. C. *J. Phys. Chem. B* **2010**, *114*, 11620−11627.

(30) Humphrey, W.; Dalke, A.; Schulten, K. *J. Mol. Graph.* **1996**, *14*, 33−38 ; 27−38.

(31) Brooks, B. R.; Brooks, C. L., 3rd; Mackerell, A. D., Jr.; Nilsson, L.; Petrella, R. J.; Roux, B.; Won, Y.; Archontis, G.; Bartels, C.; Boresch, S.; Caflisch, A.; Caves, L.; Cui, Q.; Dinner, A. R.; Feig, M.; Fischer, S.; Gao, J.; Hodoscek, M.; Im, W.; Kuczera, K.; Lazaridis, T.; Ma, J.; Ovchinnikov, V.; Paci, E.; Pastor, R. W.; Post, C. B.; Pu, J. Z.; Schaefer, M.; Tidor, B.; Venable, R. M.; Woodcock, H. L.; Wu, X.; Yang, W.; York, D. M.; Karplus, M. *J. Comput. Chem.* **2009**, *30*, 1545−1614.

(32) Hu, W. P.; Huang, L. Y.; Kuo, T. C.; Hu, W. W.; Chang, Y.; Chen, C. S.; Chen, H. C.; Chen, W. Y. *Anal. Biochem.* **2012**, *423*, 26−35.

(33) Wang, H.; Chen, S.; Li, L.; Jiang, S. *Langmuir* **2005**, *21*, 2633−2636.

(34) Piliarik, M.; Bockova, M.; Homola, J. *Biosens. Bioelectron.* **2010**, *26*, 1656−1661.